Title

Micro RNA detection in long-term fixed tissue of cortical glutamatergic pyramidal neurons after targeted laser-capture neuroanatomical microdissection

Authors

Herai, Roberto R
Stefanacci, Lisa
Hrvoj-Mihic, Branka
et al.

Publication Date

2014-09-01

DOI

10.1016/j.jneumeth.2014.06.028

Peer reviewed

Published in final edited form as:
J Neurosci Methods. 2014 September 30; 0: 76–82. doi:10.1016/j.jneumeth.2014.06.028.

Micro RNA detection in long-term fixed tissue of cortical glutamatergic pyramidal neurons after targeted laser-capture neuroanatomical microdissection

Roberto R. Herai[#1], **Lisa Stefanacci**[#2], **Branka Hrvoj-Mihic**[2], **Thanathom Chailangkarn**[1], **Kari Hanson**[2], **Katerina Semendeferi**[2,3,4,*], and **Alysson R. Muotri**[1,3,4,*]

[1]University of California San Diego, School of Medicine, Department of Pediatrics/Rady Children's Hospital San Diego, Department of Cellular & Molecular Medicine, Stem Cell Program, La Jolla, CA 92093, MC 0695, USA.

[2]University of California San Diego, Department of Anthropology, 9500 Gilman Drive, La Jolla, CA, 92093, USA.

[3]Center for Academic Research and Training in Anthropogeny (CARTA), University of California, San Diego, 9500 Gilman Drive, La Jolla, CA 92093. USA.

[4]Neuroscience Graduate Program, University of California San Diego, 9500 Gilman Drive, La Jolla, CA 92093, USA.

[#] These authors contributed equally to this work.

1. Introduction

Formalin-fixation (FF) is the standard and in some cases the only method for histological tissue preparation when long-term preservation is necessary. For this reason, FF samples are more widely available compared to frozen samples, and are often associated with more extensive clinical records and follow-up information (Yost et al. 2012). Although less optimal for immunohistochemistry assays compared to frozen samples, FF avoids the formation of ice crystals within the cells that usually affect cellular morphology and tissue architecture (Bedewi and Miller 2013) and is thus advantageous for the visualization and identification of specific cell types. Identification of specific cell types is crucial in genetic studies, since different cells have distinct genetic signatures, which becomes in particular important when analyzing complex tissues, such as the nervous system (Muotri and Gage 2006).

[*]To whom correspondence should be addressed: Dr. Alysson R. Muotri (muotri@ucsd.edu) or Dr. Katerina Semendeferi (ksemende@ucsd.edu).
rherai@ucsd.edu (R.H. Herai), branka_hrvoj@yahoo.com (B. Hrvoj-Mihic), tchailan@ucsd.edu (T. Chailangkarn), prim8brains@gmail.com (K. Hanson), ksemende@ucsd.edu (K. Semendeferi), muotri@ucsd.edu (A.R. Muotri).

A challenging problem with long-term FF samples, however, is the extraction of sufficient amounts of intact genetic material, including messenger RNA, because of its rapid degradation over time (van Maldegem et al. 2008). In contrast, small RNAs have a higher chance of surviving in long-term FF samples, and represent an alternative for genetic analysis associated with specific cell types (Culpin et al. 2013). These small molecules, such as micro RNAs (miRNAs), play an important role as postranscriptional repressors of gene activity, that tends to be tissue- and cell-type specific, especially in the nervous system (Smirnova et al. 2005; Mattick and Makunin 2006; Xu et al. 2011). Compromised miRNA profiles exist in several neurologic disorders, including Alzheimer's, Parkinson's, Huntington's disease, and certain types of dementia(Gascon and Gao 2012; Hsu et al. 2012). Thus, the challenge is to use the availability of FF samples to analyze the genetic architecture of specific cell types, focusing on their miRNA profiles. Although laser-capture microdissection (LCM) and RNA extraction are common techniques, they have not successfully been used together on long-term FF samples to target a specific cell type. Messenger RNA and miRNA from FF samples were previously extracted from cells, but the population comprised highly heterogeneous cell types (Li et al. 2013a), even when the analysis focuses on long-term FF tissue (Ribeiro-Silva et al. 2007). Morphologic and genetic analysis have been applied to specific cell types using LCM, but the cells were collected from newly FF samples (Jin et al. 2003), and so RNA degradation over time did not apply.

Here, we describe a method for extracting small RNAs from samples that were stored in formalin for several years. To demonstrate the applicability of the method, we used two samples from different parts of postmortem brain tissue. One sample (S1)comes from the cortex of a brain stored in formalin for over 21 years, in which wealso targeted neocortical pyramidal neurons, representing the most common morphological type of neuron in the cortex. For this sample, we then used LCM to collect pyramidal neurons specifically from supragranular cortical layers (layers II/III). Another sample (S2) corresponds to a mixed population of cortical and subcortical cells from the brain previously stored in formalin for over 6.5 years and then paraffin embedded for more 20 years. For both samples, we extracted small RNAs for high throughput sequencing (HTS) and bioinformatics analysis for small RNA detection, including several miRNAs. Our strategy is the first proof-of-principle demonstration that LCM coupled with HTS can be applied to long-term FF brain samples to analyze molecular aspects of neuronal identity.

2. Materials and methods

2.1. FF samples

Two brain samples from long-term FF tissue were utilized. One sample (S1) was comprised of a series of cortical sections obtained from the brain of a 31 year-old male fixed in formalin for 21 years.The postmortem interval for fixation was 28.5 hoursfor the S1 sample. Prior to sectioning, small (3 × 3 × 3 mm) blocks of tissue from S1 wascryoprotected by immersion in a series of sucrose solutions in phosphate buffer (10%, 20%, and 30%). The blocks were sectioned at a thickness of 10μm in a cryostat, and sections were placed onto glass slides (Fig. 1A). The second sample (S2) consisted of a series of cortical and subcortical sections obtained from a brain of a 16.5 year-old malepreviously stored in

formalin for over 6.5 years and then paraffin embedded for more 20 years. S2 was preserved by immersion in a solution of 4% formalin no more than 24 hours after the individual's death. The brain was embedded in paraffin, sectioned at 20μm in the coronal plane, and then stored at room temperature.

Additional information for sample characterization becomes necessary for studies focusing on comparing different sources of material. Here, our aim is to demonstrate that it is feasible to rescue small RNA from long-term fixed samples.The use of brain tissue subjects used in this research were approved by UC San Diego, Environment, Health and Safety (authorization number R1050), and covers inherently subject permission/authority.

2.2. Neuroanatomical identification and laser-capture microdissection

For the cortical S1 sample, sections of FF tissue were stained with a 0.25% concentration of thionin for the visualization of cells, and dehydrated in xylenes. The staining allowed for identification of the typical six-layered cellular organization of the cortex (layers I to VI; Fig. 1A). We were thus able to target individual cells based on their layer affiliation, and we focused specifically on supragranular cortical layers (layers II/III). Supragranular layers were easily distinguishable in the sections; they are bordered superiorly by an acellular layer I and inferiorly by a thin granular layer IV.

Layers II/III included pyramidal neurons and glia cells. Pyramidal neurons were distinguished from glia based on their larger size, the presence of a large nucleus with a distinct nucleolus, and an ovoid/pyramidal-shaped soma (Sherwood et al. 2006; Barger et al. 2012). Under microscopic guidance, individual pyramidal neurons from S1 were thus identified and captured using the ArcturusPixcellI LCM system for LCM (ArcturusBioscience Inc., Mountain View, CA), under 20x magnification.The optimal section thickness for cell capture was 10 microns and the minimal spot size was focused to 7.5 microns. Pyramidal neurons were collected in cryovials in preparation for RNA extraction (Fig. 1B). We manually selected and laser-capturedeach of the 5,000 layer II/III cortical pyramidal neurons. They were collected across seven individual tissue sections, representing an average of 714 collected neurons per section. Although based on a specific cellular morphology, laser capture microdissection can collect cell fragments that are over the desired cells to be collected, reducing but not compromising the purity of the dissected material.

For the S2, a paraffin-embedded 20μm thick tissue section was dissected along the midline and one hemisphere from the section in its entirety - including cortex and subcortical structures, containing all neuronal morphotypes as well as glial cells - was submitted for RNA extraction and further analyses. S2 was not subjected to LCM.

2.3. Small RNA extraction and isolation for HTS

Pyramidal neurons collected from S1 and mixed population from S2were subjected to standard procedures to minimize the exposure to high RNAse activity and purified for RNA extraction (Fig. 1B). Both samples were then processed for total RNA extraction using Recoverall Total Nucleic Acid Isolation for FFPE (Ambion, Life Technology, USA)

according to the manufacturer's protocol. The initial paraffin removal step was omitted in S1, since the sample was FF, but not paraffin-embedded.

To generate the small RNA libraries from cells of both S1 and S2 samples, isolation of small RNA was performed by cutting out gel bands between 90 and 110 nt markers. Quantification after cloning was performed using Envision Multilabel Reader 2013 from PerkinElmer (Santa Clara, CA). Small RNA cloning was performed using Illumina's Digital Gene Expression kit (v1.5). In this procedure, a 3′ PCR adapter sequence is first ligated to RNA, followed by ligation of a 5′ PCR adapter containing a barcode sequence. This barcode is used for multiplex sequencing both to reduce sequencing expense and to minimize library contamination from other cloned libraries. The RNA is then reverse-transcribed and amplified using 12 cycles of PCR. A short PCR extension time enriches for small PCR products that include miRNAs. Small RNAs are isolated by size using a 7% acrylamide gel, and multiplexed libraries are sequenced using Illumina GA2 sequencing machine. The ~5,000 collected pyramidal neuronsfrom S1and the mix population of cells S2 whereboth subjected to Illumina HTS, generating a total of 3,070,659 and 8,943,171 short single reads with a length of 36 nucleotides long, respectively.Read length of 36 nt is long enough to recognize small molecules since they are normally 15-30 bases long (smallRNAs including microRNAs), and sequencing beyond this point only sequences the adapters. PCR adapters for amplification are removed by software and remaining sequence is sufficient for small RNA identification. Similar approach for small RNA sequencing of 36 nt reads was used by different analysis, including functional studies of Ago1 proteins of microRNA pathway (Yamakawa et al. 2014), detection of small RNAs in Human Herpesvirus 6B (Tuddenham et al. 2012) and different in expression of smallRNAs from human left and right atrial (Hsu et al. 2012).

2.4. Bioinformatics analysis of HTS data for miRNA recovery

The sequenced small RNA libraries were analyzed using a suite of bioinformatics software (Fig. 1C). For quality control, raw data were first filtered using the software NGS QC Toolkit (Patel and Jain 2012). This step takes into consideration read quality and sequence contamination with different types of artifacts, such as sequencing amplicons or fragments that are too short. High quality reads were then mapped against the human reference genome (UCSC Hg19) with a fast and accurate short-read mapping software, Bowtie2 (Langmead and Salzberg 2012). The mapping step followed an incremental approach in which filtered reads were mapped without any mismatches (m=0). Those unmapped reads were then mapped back again, allowing one mismatch (m=1), and then two mismatches (m=2). This strategy allowed us to handle base-modifications caused by the RNA degradation of fixed samples, taking also into account those modifications caused by biological factors, or by sample manipulation. Then, genomic coordinates for the read-mappings were referenced to the known small RNAs from human ENSEMBL database, which contains several distinct families of small non-conding RNAs, including piwi-interacting RNAs (piRNA), small nucleolar RNAs (snoRNA) and miRNAs coordinates, also annotated in miRBase, the most complete miRNA repository database. Statistical expression analysis was not performed. Samples were based on long-term FF samples having a small concentration of RNA. The limited small number of collected cells from S2 and the fact that both samples are long-term

FF tissuesthat have high level of RNA degradation over time can interfere on wrongly modulating transcriptome expression levels. Although it is possible to detect small RNAs, quantification analysis is hard to be connected with cell transcriptome expression because degradation levels of different FF samples are not homogeneous over the time.

3. Results

We successfully detected small RNA insequenced samples from ~5,000 pyramidal neurons from S1 and mix population of cells S2, both stored in long-term FF postmortem brain tissue. The quantification procedure (see Material and Methods section) for the amount of isolated and cloned RNA revealed a total of 0.565 ng and 0.34 ng of extracted RNA for the cells from samples S1 and S2, respectively.

For the small RNA HTS of sequenced samples having cells from S1 and S2, the bioinformatics pipeline for data quality check revealed 18,539 and 970,178 high-quality reads, respectively. This is a significantly reduced number of reads compared to sequencing newly FF samples (Li et al. 2013). Mapping those high-quality reads against the human reference genome (Fig. 2A – Genome alignment) yielded a total of 71% successfully mapped reads for data from LCM cells of S1, and 44% of successfully mapped readsfromS2 data against the same genome (Fig. 2B – Genome alignment). According to our approach, the mapped reads from cells of S1 and S2 distributed over the genome with different numbers of absolute mismatches (m). Most of reads from LCM S1 sample have 0 mismatches (m=0), 61% on total, 1% have one exact mismatch (m=1) and the other 37% mappings have 2 mismatches (m=2) (Fig. 2A – Alignment mismatches). Similarly, the mapping of S2 data was distributed over the genome with most of reads having m=0, 65% on total, 26% having m=1 and the other 9% mappings with m=2 (Fig. 2B - Alignment mismatches). The computational approach was designed for only 1 and 2 mismatches for 36 nt sequenced libraries. Allowing more than two mismatches significantly increases the number of repetitive alignments over different classes of smallRNAs and, consequently, the number of detected false-positive molecules.

Annotation coordinates of the ENSEMBL database were then compared with those mapped reads against the human reference genome, yielding a total of 1,326(Fig. 2A - ncRNA) and 3,476 (Fig. 2B - ncRNA) identified ncRNAs for pyramidal neurons from S1 and mixed population of cells from S2, respectively. Within these mappings, considering up to 2 mismatches, in S1 cells we identified 29 annotated miRNA (Supplemental Table S1a), 83 piRNA (Supplemental Table S2a) and 1,505 other ncRNA (Supplemental Table S3a).Formappings of S2 data over genome, applying exactly the same computational approach, we identified 89 annotated miRNA (Supplemental Table S1b), 176 piRNA (Supplemental Table S2b) and 3,219 other ncRNA (Supplemental Table S3b). Some of these detected sRNA were found to be common in both pyramidal cells from S1 and mixed cells from S2, such as 15 miRNA (Fig. 2D), 12 piRNA (Fig. 2E) and 584 other ncRNA (Fig. 2F).

4. Discussion

A significant contribution of our methodology was to systematically uncover miRNAs and other families of small RNAs using cutting-edge genomic and neuroanatomic techniques to target a specific morphologic class of neurons, extracted from a specific laminar site. Although RNA extraction has been performed to some degree on FF tissue, the most common method for brain preservation, it is still challenging to isolate genetic material since long-term fixation degrades messenger RNA over time. Small RNA, such as miRNA and piRNA, however, does not degrade to the same degree as messenger RNA(Li et al. 2007; Ravo et al. 2008).

In this study, we demonstrated theuse of LCM to collect cortical pyramidal neurons specifically from supragranular cortical layers (layers II/II), and compared the results with a sample of mixed populations of cells from cortical and subcortical postmortem brain tissues. The application of LCM focused on pyramidal neurons since they are the most common morphologic type of neuron in the cortex, they form the basic units of cortical microcircuitry, and they often display morphologic modifications associated with neurologic disorders (Gascon and Gao 2012). Similarly, deficiencies in miRNA activity are described in several disorders and may represent a compromise in regulatory mechanisms underlying the appearance of neuronal pathologies (Gascon and Gao 2012).

The cells from S1 and S2 samples were treated for RNA extraction and isolation, and we successfully recovered miRNAs. This was accomplished by using HTS on isolated RNA, so that we were able to manage the high degradation levels previously observed in long-term FF samples (van Maldegem et al. 2008). In this way, we were able to rescue thousands of high quality short RNA fragments. Our *in silico*incremental approach based on the number of mismatches specifically mapped the reads against different classes of small RNA. Some of these transcripts includes miRNA molecules that were detected in both targeted pyramidal neurons from S1 and mixed population of cells from S2 (Fig. 2C), such as the brain-specific miRNA hsa-mir-9-3 (Liu et al. 2010) that is only expressed in the nervous system; hsa-mir-206, which targets the BDNF gene that is involved in several neural pathways, including the survival, growth, and maturation of neurons and synapses (Chen et al. 2013); has-mir-342, which targets the EVL gene that is related to control processes dependent on cell polarity such as axon outgrowth and guidance(Dent et al. 2011); and hsa-mir-148b, which targets to NPTX2 gene that is involved in excitatory synapse formation (Bjartmar et al. 2006).

Although we did not use of the most recent method for RNA library preparation, we were also able to detect expression of a miRNA, hsa-mir-155, that was not previously described to be expressed in neurons.It has only been shown that has-mir-155 is expressed by other human nervous cells, including glial (Cardoso et al. 2012) and astrocytes (Tarassishin et al. 2011). To support the evidence that hsa-mir-155 is expressed by neurons since its expression was detected in long-term FF samples that are prone to degradation, we analyzed and independent smallRNA sequencing databank, generated with HTS of FAC-sorted (fluorescence-activated cell sorted) neuronsobtained by the induced pluripotent stem cell (iPS) technology(Marchetto et al. 2013).Applying a bioinformatics approach based on non-

redundant sequence alignment (reads that align exclusively in one genome locus), we found expression of hsa-mir-155 in two independent biological replicates ofiPS-derived neurons (Fig. 3G). This miRNA can represent, although never previously reported for neurons, an important candidate for studies related with neuron phenotype since one possible target for hsa-mir-155 is the JARID2 gene, that is involved in regulating cell proliferation and neural tube formation (Walters et al. 2013).

Additionally, some identified miRNAs we detected in cells from both S1 and S2 samples are involved with genes that act in several cellular processes (Fig. 2C), such as hsa-mir-99a, which targets the MTOR gene, regulating cell growth, cell proliferation, cell motility, cell survival, protein synthesis, and transcription (Chen et al. 2013) and hsa-mir-25, which targets the CALN1 gene, a brain-specific gene that is involved in calcium signaling transduction by binding calcium ions inside cells (Wu et al. 2001). These detected miRNA potentially target specific genes are directly involved with brain regulation and activity, suggesting that even in long-term FF samples we can perform genetic studies of specific populations of cells. However, some brain specific miRNAs, such as has-mir-124 and has-mir-9(Xu et al. 2011), were not detected by our bioinformatics analysis. Thus, RNA degradation in long-term FF samples could be a potential explanation and limitation of the current technique. Although it was also reported that miRNA can be up to 10x more stable than messenger RNAs (Gantier et al. 2011), it is still unclear how stability varies between different miRNA molecules. Recent findings suggests that miRNA stability can be modulated by miRNA expression level and several other cohorts of factors that include miRNA targets, small RNA degradation pathways, nucleotide content, evolution, associated disease, and environmental factors (Kai and Pasquinelli 2010; Li et al. 2013b).

These results from LCM pyramidal neurons of S1 and from a mixed population of cells from S2 can be expanded to detect new classes of small RNA, or types of brain-specific miRNA as we did show for the hsa-mir-155 in neurons. For the collected pyramidal neurons from S1 sample, for example, increasing the number of laser-captured neurons could further increase the number of sequenced reads from the 18,539 high-quality reads that we obtained for small RNA detection. Increasing the number of laser-captured neurons could also increase the possibility of recovering sparser miRNAs, which might be more affected by the degradation and low concentration of RNA. In the mixed population of cells from S2, although more than 89% of sequenced readshave low-quality (removed after filtering step), the higher amount of high-quality reads compared to cells from S1 sample,enabled us to detect more molecules (2,615 ncRNA)that were not detected in data from S1 sample (Fig. 3G). Although in this study we focused specifically on pyramidal neurons when using LCM, the method can also be used to study other cell types based on known anatomic criteria. Furthermore, we can also take advantage of the wide availability of long-term FF samples since they often have a more extensive clinical follow-up (Yost et al. 2012), opening a possibility to examine genetic aspects of various pathologies for which fresh samples are not available and cell morphology is necessary.

We plan to apply this approach to multiple comparisons involving various cell types and cortical areas in our future experiments since our aim, as a proof-of-principle only, was to demonstrate that it is possible to rescue small RNA from long-term fixed samples. Although

it could be interesting to compare frozen fixed with fresh tissue samples, such direct comparison is not feasible methodologically. FF tissues are stored in brain banks either frozen or fixed and thus using samples from different brains or different parts of brain would have challenges of its own due to variability.Although streamlining the technique involved considerable effort, efficient application of our method is feasible using state of the art LCM technology, and thus complimentary and even advantageous to other approaches. As a proof-of-principle, we demonstrate that our method can even work for a mixed population of cells from the brain, or for a small population of ~5,000 cells. However, by increasing the number of collected cells and the number of analyzed samples we could increase the number of detected microRNAs as well as the confidence of results. This could also allow for correlation of the number of collected cells with the number of detectable microRNAs. Taking into account that formalin-fixation has been a standard for decades and in some cases is the only method for histological tissue preparation when long-term preservation is necessary, our method has several potential applications even with a limited number of detected smallRNAs. Studies of rare neurological disease, for example, can be performed to detect small molecules when the tissue material is only available in formalin fixed material. The method can be useful in conducting evolutionary studies, where few available comparative specimens hinder the analyses of uniquely human regulatory aspects associated with brain expansion. Our method can be further expanded for the analysis of other rare and endemic disease, and promote additional analyses of FF pathological specimens which have been kept in formalin for several decades.

5. Conclusion

Previous studies involving small RNA analysis at the nucleotide resolution using FF samples were based on RNA extraction of highly heterogeneous populations of cells, as we did for the mixed population of cells from S2 sample, or originated from freshly FF samples. This is the first study to analyze a specific class of cells from long-term FF samples. Extraction and analysis of small RNAs from a target population of neurons opens the possibility for obtaining genetic information from the long-term FF specimens in which mRNA and long non-coding RNA are unlikely to be rescued in sufficient amounts for quantitative analyses. Additionally, our results reveal that the entireprocedure involving LCM, small RNA extraction using HTS, and bioinformatics analysis can be applied to samples of varying fixation times, even those over 21 years as we did for pyramidal cells from S1 sample. Even with the use of such long-term fixed samples, we found, for the first time, that hsa-mir-155 is expressed in analyzed samples from FF brain tissue. This evidence of expression was used to design an *in silico* experiment to confirm that hsa-mir-155 is expressed in neurons, supported by two biological replicates of sequenced small RNAsfrom cultured neurons(Marchetto et al. 2013). This approach has the potential to contribute substantially to the study of neuronal diversity in humans and other primates and to understanding the molecular pathology underlying neurological diseases, revealing true the molecular players in specific neuronal types.

Supplementary Material

Refer to Web version on PubMed Central for supplementary material.

Acknowledgments

The work was supported by grants from the Kavli Institute for Brain and Mind at UC San Diego, from the National Institutes of Health through the NIH Director's New Innovator Award Program, 1-DP2-OD006495-01, P01 NICHD033113 and from the International Rett Syndrome Foundation (IRSF grant# 2915). R.H.H. is an IRSF Fellow (IRSF grant# 2925) and B.H.M. is supported by the Rita L. Atkinson Graduate Fellowship.

References

Barger N, Stefanacci L, Schumann CM, Sherwood CC, Annese J, Allman JM, et al. Neuronal populations in the basolateral nuclei of the amygdala are differentially increased in humans compared with apes: A stereological study. J Comp Neurol. 2012; 520(13):3035–54. [PubMed: 22473387]

Bedewi AEL, Miller L. Discrimination Between Paraffin-Embedded and Frozen Skin Sections Using Synchrotron Infrared Microspectroscopy. Int J Pept Res Ther. Aug 2.2013

Bjartmar L, Huberman AD, Ullian EM, Rentería RC, Liu X, Xu W, et al. Neuronal pentraxins mediate synaptic refinement in the developing visual system. J Neurosci. Jun 7; 2006 26(23):6269–81. [PubMed: 16763034]

Cardoso AL, Guedes JR, Pereira de Almeida L, Pedroso de Lima MC. miR-155 modulates microglia-mediated immune response by down-regulating SOCS-1 and promoting cytokine and nitric oxide production. Immunology. Jan; 2012 135(1):73–88. [PubMed: 22043967]

Chen A, Xiong L-J, Tong Y, Mao M. Neuroprotective effect of brain-derived neurotrophic factor mediated by autophagy through the PI3K/Akt/mTOR pathway. Mol Med Rep. Oct; 2013 8(4): 1011–6. [PubMed: 23942837]

Culpin RE, Sieniawski M, Proctor SJ, Menon G, Mainou-Fowler T. MicroRNAs are suitable for assessment as biomarkers from formalin-fixed paraffin-embedded tissue, and miR-24 represents an appropriate reference microRNA for diffuse large B-cell lymphoma studies. J Clin Pathol. Mar 1; 2013 66(3):249–52. [PubMed: 23172553]

Dent EW, Gupton SL, Gertler FB. The growth cone cytoskeleton in axon outgrowth and guidance. Cold Spring Harb Perspect Biol. Mar.2011 3(3)

Gantier MP, McCoy CE, Rusinova I, Saulep D, Wang D, Xu D, et al. Analysis of microRNA turnover in mammalian cells following Dicer1 ablation. Nucleic Acids Res. Jul 1; 2011 39(13):5692–703. [PubMed: 21447562]

Gascon E, Gao F-B. Cause or Effect: Misregulation of microRNA Pathways in Neurodegeneration. Front Neurosci. Frontiers. Jan 9.2012 6:48.

Hsu J, Hanna P, Van Wagoner DR, Barnard J, Serre D, Chung MK, et al. Whole genome expression differences in human left and right atria ascertained by RNA sequencing. Circ Cardiovasc Genet. Jun 1; 2012 5(3):327–35. [PubMed: 22474228]

Jin L, Majerus J, Oliveira A, Inwards CY, Nascimento AG, Burgart LJ, et al. Detection of Fusion Gene Transcripts in Fresh-Frozen and Formalin-Fixed Paraffin-Embedded Tissue Sections of Soft-Tissue Sarcomas After Laser Capture Microdissection and RT-PCR. Diagnostic Mol Pathol. 2003

Kai, ZS.; Pasquinelli, AE. Nat Struct Mol Biol. Vol. 17. Nature Publishing Group; Jan. 2010 MicroRNA assassins: factors that regulate the disappearance of miRNAs; p. 5-10.

Langmead, B.; Salzberg, SL. Nat Methods. Vol. 9. Nature Publishing Group, a division of Macmillan Publishers Limited; May. 2012 Fast gapped-read alignment with Bowtie 2; p. 357-9.All Rights Reserved

Li J, Smyth P, Flavin R, Cahill S, Denning K, Aherne S, et al. Comparison of miRNA expression patterns using total RNA extracted from matched samples of formalin-fixed paraffin-embedded (FFPE) cells and snap frozen cells. BMC Biotechnol. Jan.2007 7(1):36. [PubMed: 17603869]

Li X, Lu Y, Chen Y, Lu W, Xie X. MicroRNA profile of paclitaxel-resistant serous ovarian carcinoma based on formalin-fixed paraffin-embedded samples. BMC Cancer. Jan.2013 a 13(1):216. [PubMed: 23627607]

Li Y, Li Z, Zhou S, Wen J, Geng B, Yang J, et al. Genome-wide analysis of human microRNA stability. Biomed Res Int. Jan.2013 b 2013:368975. [PubMed: 24187663]

Liu, D-Z.; Tian, Y.; Ander, BP.; Xu, H.; Stamova, BS.; Zhan, X., et al. J Cereb Blood Flow Metab. Vol. 30. Nature Publishing Group; Jan 2. 2010 Brain and blood microRNA expression profiling of ischemic stroke, intracerebral hemorrhage, and kainate seizures; p. 92-101.

Van Maldegem F, de Wit M, Morsink F, Musler A, Weegenaar J, van Noesel CJM. Effects of processing delay, formalin fixation, and immunohistochemistry on RNA Recovery From Formalin-fixed Paraffin-embedded Tissue Sections. Diagn Mol Pathol. Mar; 2008 17(1):51–8. [PubMed: 18303406]

Marchetto, MCN.; Narvaiza, I.; Denli, AM.; Benner, C.; Lazzarini, TA.; Nathanson, JL., et al. Nature. Vol. 503. Nature Publishing Group; Nov 28. 2013 Differential L1 regulation in pluripotent stem cells of humans and apes; p. 525-9.

Mattick JS, Makunin IV. Non-coding RNA. Hum Mol Genet. Apr 15.2006 (15 Spec No):R17–29. [PubMed: 16651366]

Muotri AR, Gage FH. Generation of neuronal variability and complexity. Nature. Jun 29; 2006 441(7097):1087–93. [PubMed: 16810244]

Patel, RK.; Jain, M. NGS QC Toolkit: a toolkit for quality control of next generation sequencing data. In: Liu, Z., editor. PLoS One. Vol. 7. Public Library of Science; Jan. 2012 p. e30619

Ravo, M.; Mutarelli, M.; Ferraro, L.; Grober, OMV.; Paris, O.; Tarallo, R., et al. Lab Invest. Vol. 88. United States and Canadian Academy of Pathology, Inc.; Apr 25. 2008 Quantitative expression profiling of highly degraded RNA from formalin-fixed, paraffin-embedded breast tumor biopsies by oligonucleotide microarrays; p. 430-40.

Ribeiro-Silva A, Zhang H, Jeffrey SS. RNA extraction from ten year old formalin-fixed paraffin-embedded breast cancer samples: a comparison of column purification and magnetic bead-based technologies. BMC Mol Biol. Jan.2007 8:118. [PubMed: 18154675]

Sherwood CC, Stimpson CD, Raghanti MA, Wildman DE, Uddin M, Grossman LI, et al. Evolution of increased glia-neuron ratios in the human frontal cortex. Proc Natl Acad Sci U S A. Sep 12; 2006 103(37):13606–11. [PubMed: 16938869]

Smirnova L, Gräfe A, Seiler A, Schumacher S, Nitsch R, Wulczyn FG. Regulation of miRNA expression during neural cell specification. Eur J Neurosci. Mar; 2005 21(6):1469–77. [PubMed: 15845075]

Tarassishin L, Loudig O, Bauman A, Shafit-Zagardo B, Suh H-S, Lee SC. Interferon regulatory factor 3 inhibits astrocyte inflammatory gene expression through suppression of the proinflammatory miR-155 and miR-155*. Glia. Dec; 2011 59(12):1911–22. [PubMed: 22170100]

Tuddenham L, Jung JS, Chane-Woon-Ming B, Dölken L, Pfeffer S. Small RNA deep sequencing identifies microRNAs and other small noncoding RNAs from human herpesvirus 6B. J Virol. Feb; 2012 86(3):1638–49. [PubMed: 22114334]

Walters, ZS.; Villarejo-Balcells, B.; Olmos, D.; Buist, TWS.; Missiaglia, E.; Allen, R., et al. Oncogene. Macmillan Publishers Limited; Feb 25. 2013 JARID2 is a direct target of the PAX3-FOXO1 fusion protein and inhibits myogenic differentiation of rhabdomyosarcoma cells.

Wu Y-Q, Lin X, Liu C-M, Jamrich M, Shaffer LG. Identification of a Human Brain-Specific Gene, Calneuron 1, a New Member of the Calmodulin Superfamily. Mol Genet Metab. 2001; 72(4):343–50. [PubMed: 11286509]

Xu X-L, Zong R, Li Z, Biswas MHU, Fang Z, Nelson DL, et al. FXR1P but not FMRP regulates the levels of mammalian brain-specific microRNA-9 and microRNA-124. J Neurosci. Sep 28; 2011 31(39):13705–9. [PubMed: 21957233]

Yamakawa N, Okuyama K, Ogata J, Kanai A, Helwak A, Takamatsu M, et al. Novel functional small RNAs are selectively loaded onto mammalian Ago1. Nucleic Acids Res. Mar 13.2014 :gku137.

Yost SE, Smith EN, Schwab RB, Bao L, Jung H, Wang X, et al. Identification of high-confidence somatic mutations in whole genome sequence of formalin-fixed breast cancer specimens. Nucleic Acids Res. Aug 1.2012 40(14):e107. [PubMed: 22492626]

Highligths

- We detected microRNA from formalin fixed brain stored for over decades.
- Pyramidal shaped neurons can be collected by laser-capture microdissection.
- Sufficient smallRNA can be extracted from long-term laser-captured neurons.
- RNA from collected neurons can be subjected to smallRNA high throughput sequencing.

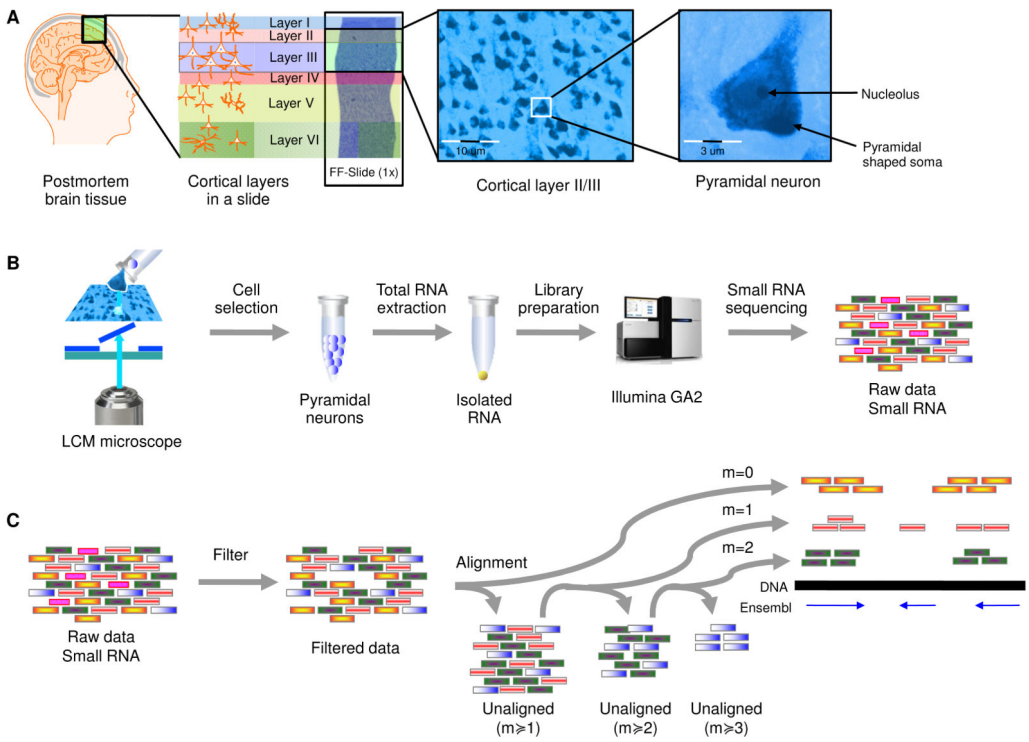

Figure 1. Laser-capture approach for pyramidal neurons isolation for miRNA extraction and analysis

A, Sectioned postmortem brain tissue from a FF brain with the six cortical layers in a slide: layer I, layer II, layer III, layer IV, layer V, layer VI. **B**, Laser-captured pyramidal neurons in a cap, for RNA isolation and Illumina GA2 sequencing machine generating short fragments (raw reads) of small RNA.**C**, Raw reads are filtered and then mapped against human reference genome (Hg 19) considering zero mismatch (m=0), one mismatch (m=1) and two mismatches (m=2), using the raw reads and then the unmapped set of reads having at least one mismatch (m≥1) and two mismatches (m≥2), respectively. The final set of unmapped reads is composed by those reads having at least three mismatches (m≥3) compared to the reference genome.

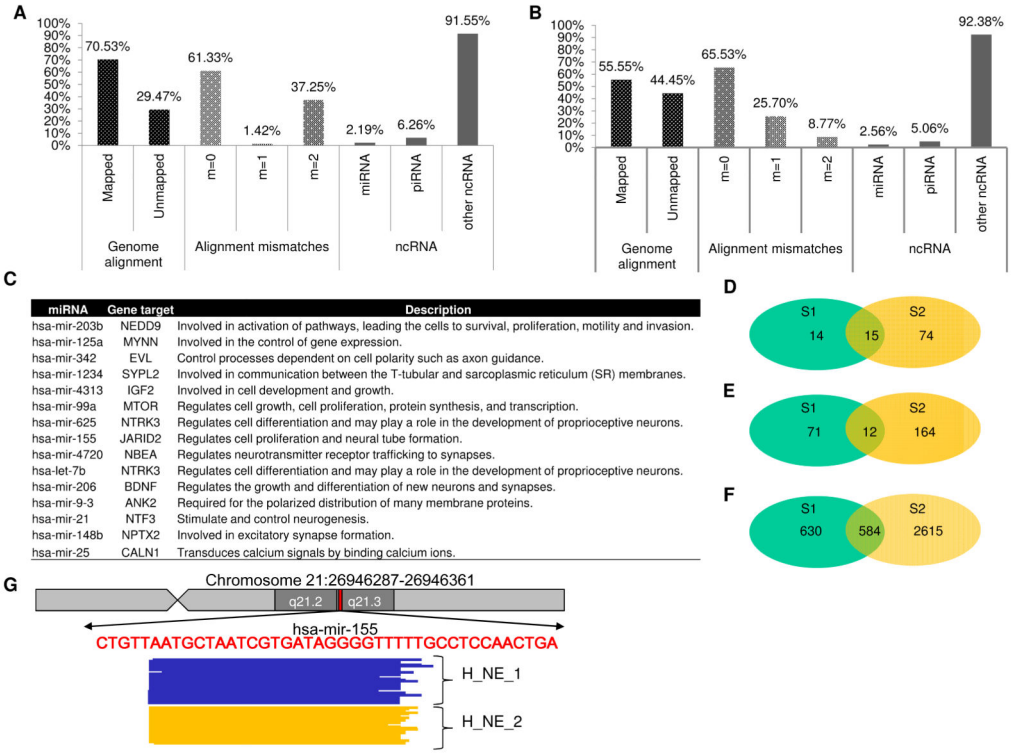

miRNA	Gene target	Description
hsa-mir-203b	NEDD9	Involved in activation of pathways, leading the cells to survival, proliferation, motility and invasion.
hsa-mir-125a	MYNN	Involved in the control of gene expression.
hsa-mir-342	EVL	Control processes dependent on cell polarity such as axon guidance.
hsa-mir-1234	SYPL2	Involved in communication between the T-tubular and sarcoplasmic reticulum (SR) membranes.
hsa-mir-4313	IGF2	Involved in cell development and growth.
hsa-mir-99a	MTOR	Regulates cell growth, cell proliferation, protein synthesis, and transcription.
hsa-mir-625	NTRK3	Regulates cell differentiation and may play a role in the development of proprioceptive neurons.
hsa-mir-155	JARID2	Regulates cell proliferation and neural tube formation.
hsa-mir-4720	NBEA	Regulates neurotransmitter receptor trafficking to synapses.
hsa-let-7b	NTRK3	Regulates cell differentiation and may play a role in the development of proprioceptive neurons.
hsa-mir-206	BDNF	Regulates the growth and differentiation of new neurons and synapses.
hsa-mir-9-3	ANK2	Required for the polarized distribution of many membrane proteins.
hsa-mir-21	NTF3	Stimulate and control neurogenesis.
hsa-mir-148b	NPTX2	Involved in excitatory synapse formation.
hsa-mir-25	CALN1	Transduces calcium signals by binding calcium ions.

Figure 2. Small RNA profile from laser-captured neurons and mixed population of cells of FF postmortem brain samples

A,Alignment characteristics of high quality reads from S1 sample: proportion of mapped and unmapped high quality reads from S1 on human reference genome (Hg19); frequency distribution of those genome mapped reads from S1 neurons considering different number of mismatches: m=0, m=11 and m=2; mapped reads from S1 neurons overlapping genomic coordinates of annotated ENSEMBL ncRNA transcripts; **B**,Alignment characteristics of high quality reads from S2 sample: proportion of mapped and unmapped high quality reads from S2 mixed population of cells on human reference genome (Hg19); frequency distribution of those genome mapped reads from S2 mixed population of cells considering different number of mismatches: m=0, m=11 and m=2; mapped reads from S2 mixed population of cells overlapping genomic coordinates of annotated ENSEMBL ncRNA transcripts. **C**, list of the fifteen common miRNA (miRNA code) to laser-captured S1 pyramidal neurons and S2 mixed population of cells. **D**, absolute number of common (15 miRNA) and specific miRNA molecules in cells from S1 (14 miRNA) and S2 (74 miRNA) samples.**E**, Absolute number of common (12 piRNA) and specific piRNA molecules in cells from S1 (71 piRNA) and S2 (164 piRNA) samples.**F**, Absolute number of common (584 ncRNA) and specific ncRNA molecules in cells from S1 (630 ncRNA) and S2 (2615 ncRNA) samples, not including those detected piRNA and miRNA molecules.**G**, Representative view of human hsa-mir-155 miRNA transcript locus (in red) located at chromosome 21 (positions 26946287-26946361 of human genome Hg19), band q21.3 (near to band q21.2) and aligned reads from two samples, H_NE_1 (yellow) and H_NE_2 (blue), downloaded from public databanks (GEO under accession number GSE47626),

corresponding to sequenced small RNA data of human neurons, generated by induced pluripotent stem cell technology (Marchetto et al. 2013).